Key Engineering Materials
ISSN: 1662-9795, Vol. 1054, pp 9-16
doi:10.4028/p-2L2smi

Submitted: 2025-08-29
Revised: 2025-12-10
Accepted: 2026-03-08
Online: 2026-05-18

Development and Evaluation of a 1.2kV SiC MOSFET-Based PTC Controller for Energy-Efficient xEV Heating Applications

Jeong-Hwan Jang[1,a], Jang-Kwon Lim[2,b*], Kalle Ilves[3,c], Ki-Sun Song[1,d], Dong-In Yang[1,e], Young-Jin Kim[1,f] and Kyu-Bong Yeon[4,g]

[1]REVOTECH, 51 Neungwon-ro, Mohyeon-eup, Cheoin-gu, Yongin-si, Gyeonggi-do, South Korea

[2]RISE Research Institutes of Sweden AB, Isafjordsgatan 2, Kista, Sweden

[3]Coherent-KISTA, Isafjordsgatan 22B, Electrum 207, Kista, Sweden

[4]KATECH Korea Automotive Technology Institute, 303 Pungse-ro, Pungse-Myeon, Cheonan-Si, Chungnam, South Korea

[a]jhjang@revotech.kr, [b*]Jang-Kwon.Lim@ri.se, [c]kalle.ilves@coherent.com, [d]kssong@revotech.kr, [e]diyang@revotech.kr, [f]yjkim@revotech.kr, [g]kbyeon@katech.re.kr

Keywords: HVAC (Heating Ventilation Air-Conditioning), SiC MOSFETs, positive temperature coefficient (PTC), negative temperature coefficient (NTC), junction temperature (T_j), heating application.

Abstract. This paper presents the development and evaluation of a 1.2 kV SiC MOSFET-based Positive Temperature Coefficient (PTC) controller designed for energy-efficient heating applications in electric vehicles (xEVs). To address the increasing demand for higher-voltage battery systems in modern xEVs, a PTC controller utilizing wide bandgap (WBG) semiconductor technology was developed. The proposed system leverages a 1.2 kV SiC MOSFET to enable high-frequency operation up to 20 kHz, thereby mitigating audible noise issues by operating beyond the human hearing range. Unlike conventional IGBT-based controllers, which exhibit significant limitations at high switching frequencies, the SiC MOSFET-based controller demonstrates reliable high-frequency operation, reduced switching losses, and improved overall efficiency. Experimental validation confirms that the proposed approach not only ensures low-noise heating operation but also enhances energy efficiency, making it a promising solution for next-generation xEV thermal management systems.

Introduction

As the adoption of electric vehicles (xEVs) continues to expand, the demand for effective and energy-efficient cabin heating systems is becoming increasingly critical. Modern xEVs rely on Heating, Ventilation, and Air Conditioning (HVAC) systems not only to maintain passenger comfort but also to ensure the safe operation of battery and electronic components through effective thermal management. Within the HVAC system, Positive Temperature Coefficient (PTC) heaters are widely used as an auxiliary heating source, especially under cold ambient conditions where heat pump efficiency drops significantly. Unlike internal combustion engine vehicles, battery electric vehicles (BEVs) do not benefit from waste heat generated by the engine and must generate heat electrically.

Conventional PTC systems employing silicon Insulated Gate Bipolar Transistors (Si-IGBTs) exhibit significant energy inefficiencies. These devices experience high conduction losses due to their inherent knee voltage characteristics and substantial switching losses resulting from long tail currents during turn-off [1,2]. In practical usage, electric taxis can experience up to a 40% reduction in available battery capacity for heating during winter, which reduces their effective driving range from 135 km to approximately 80 km per charge [3].

Such limitations highlight a fundamental barrier to the widespread adoption of xEVs in colder regions, where customer acceptance and operational feasibility are strongly influenced by heating efficiency. Moreover, as global automotive manufacturers transition toward higher-voltage battery platforms (600–1000 V and beyond) to shorten charging times and extend driving ranges, heating

controllers must be designed to operate reliably at elevated voltages while simultaneously achieving higher efficiency and reduced acoustic noise.

In response to these challenges, this work presents the design, development, and experimental evaluation of a next-generation PTC controller based on Silicon Carbide (SiC) MOSFET technology. Unlike conventional IGBTs, SiC devices can sustain high-frequency operation, enabling switching above 20 kHz to suppress audible noise and improve overall power conversion efficiency. SiC devices offer superior performance characteristics, including significantly lower switching and conduction losses, higher breakdown voltages, and excellent thermal robustness [4,5,6].

These advantages not only address the inherent drawbacks of IGBT-based PTC systems but also open the pathway for compact, lightweight, and energy-efficient heating solutions. Such improvements are especially critical in the context of electric mobility, where every increment in energy savings directly translates into extended driving range and reduced total cost of ownership. Preliminary acoustic tests indicated that when the switching frequency exceeded 20 kHz—specifically at 100 kHz—the emitted sound resembled white noise, which is imperceptible within the human audible range. This feature not only suggests the potential to resolve passenger discomfort associated with noise but also contributes directly to enhanced service quality and customer satisfaction in electric vehicle applications.

Engineering of 1200 V SiC MOSFETs for Stable Temperature Operation

Building on the need for high-efficiency and thermally robust PTC controllers, we developed and evaluated SiC MOSFET devices designed for stable temperature operation. To enhance the thermal stability of the PTC controller over operational temperatures, we employed SiC MOSFETs engineered with different on-resistance (R_{DSon}) and threshold voltage (V_{TH}) specifications. By investigating the trade-off between V_{TH} and $R_{DS(on)}$ across temperatures, we aimed to balance conduction loss and switching performance under realistic PTC load conditions. We analyzed the trade-off between conduction and switching losses in our 1200 V SiC MOSFETs, with a particular focus on the temperature dependencies of V_{TH} and R_{DSon}, as shown in Figs 1 and 2. As temperature increases, V_{TH} exhibits a negative temperature coefficient (NTC) behavior because elevated lattice temperature reduce carrier mobility in the MOS channel and enhance carrier scattering, thereby requiring a lower gate voltage to form the conducting channel. This shift can increase the risk of false turn-on or higher leakage currents. Conversely, R_{DSon} shows a positive temperature coefficient (PTC) behavior due to mobility degradation in the drift region and increased resistivity from enhanced phonon scattering, leading to higher conduction losses at elevated temperatures. Our devices maintained consistent and predictable trends in both parameters up to 175°C, enabling an optimized balance between switching speed and conduction efficiency. This favorable thermal behavior minimizes total power loss under realistic PTC load conditions and improves the controller's robustness against high ambient temperatures and transient heating environments. These results demonstrate that, with appropriate device selection and thermally aware gate-driving strategies, SiC MOSFETs can deliver stable, high-efficiency operation for next-generation xEV PTC controllers.

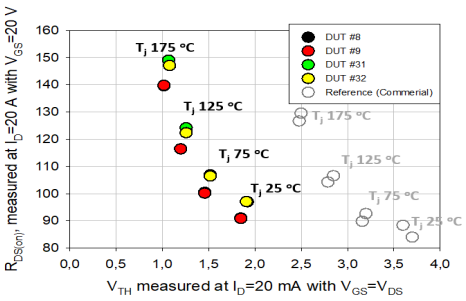

Fig. 1. Comparison of on-state resistance and threshold voltage on temperature dependency for 1200V/90mΩ SiC MOSFET.

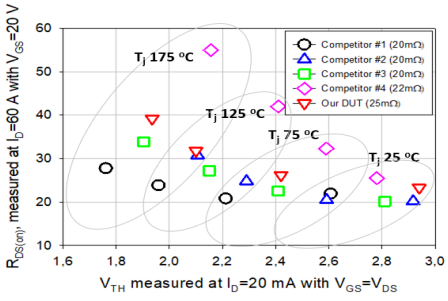

Fig. 2. Comparison of on-state resistance and threshold voltage on temperature dependency for 1200V/20mΩ SiC MOSFET.

SiC MOSFET-adopted PTC Controller Design

Leveraging the favourable device characteristics confirmed in the previous section, we developed a 1.2 kV SiC MOSFET-based PTC controller optimized for high-voltage xEV heating applications, aiming to ensure stable operation, minimize audible noise through high-frequency switching, and enhance overall energy efficiency under realistic load conditions.

The overall system architecture of the proposed PTC controller, including the application of the isolated gate driver and peripheral circuitry, is illustrated in Fig. 3. The controller was designed based on a nominal xEV battery voltage of 523 V, ensuring compatibility with practical vehicle platforms. To accommodate voltage fluctuations and transient conditions, the system was engineered to operate reliably within a wide input range of 650 V ± 150 V range. In compliance with automotive design guidelines, power semiconductor devices rated for approximately twice the nominal operating voltage were employed to guarantee safe and reliable operation.

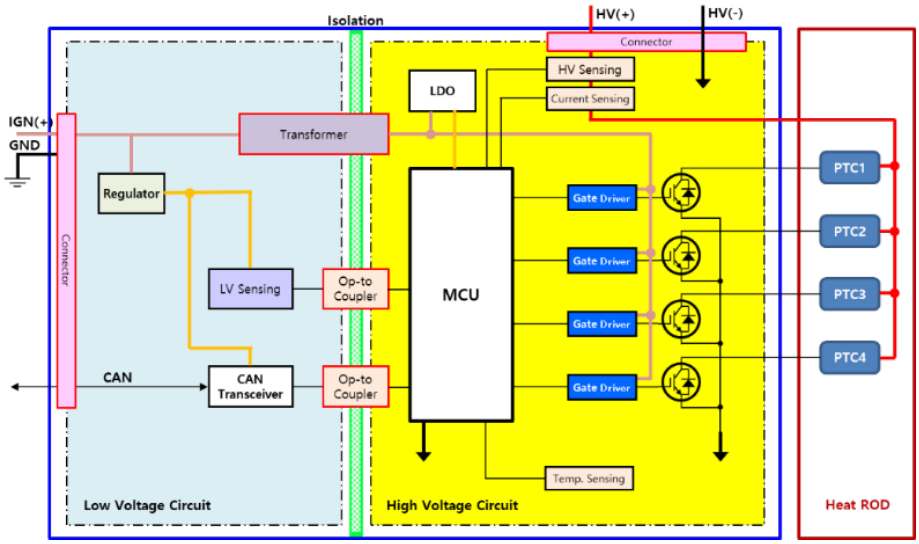

Fig. 3. Block diagram of the proposed PTC controller system architecture.

Furthermore, in order to meet the requirements of an 8 kW PTC rod, the controller was designed in accordance with the RT-curve characteristics of the PTC ceramic, as illustrated in Fig. 4. To enhance heating flexibility and user comfort, the system was implemented with a four-channel architecture, enabling independent control of heating for both the driver and individual passengers.

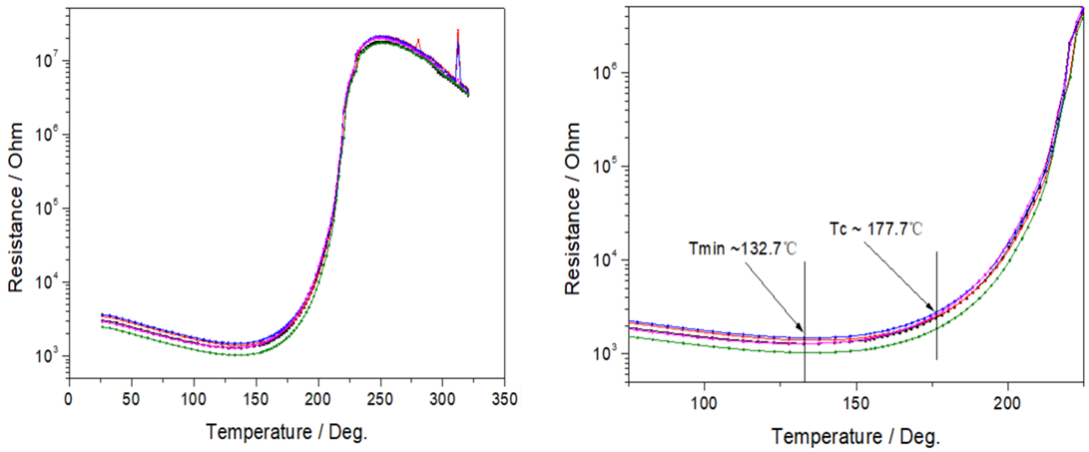

Fig. 4. RT-curve of the PTC ceramic used in the proposed 8 kW heater design.

In addition, as shown in Fig. 5, electromagnetic compatibility was evaluated through SiWAVE simulations, while mechanical and thermal reliability was analyzed using Sherlock, thereby ensuring that the proposed PTC controller was developed with both electromagnetic compliance and long-term durability in mind.

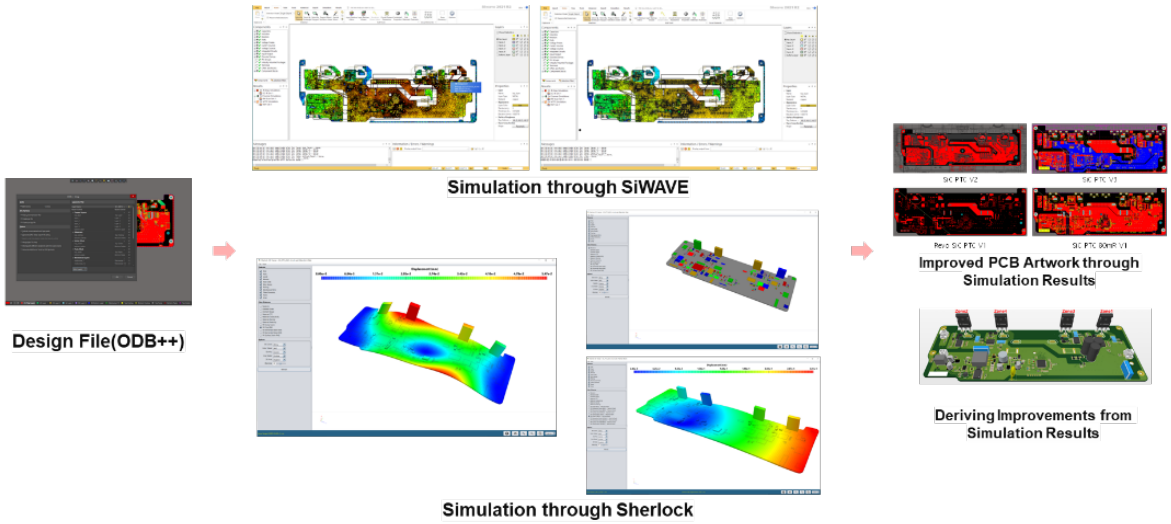

Fig. 5. PCB design validation using Siwave for EMC analysis and Sherlock for reliability evaluation.

Fig. 6 presents both the 1.2 kV SiC MOSFET device and the fabricated PTC controller prototype incorporating the device. The prototype was implemented by applying design improvements derived from preliminary test analyses, which addressed issues such as low-voltage supply, isolation distance, and gate driver performance. The controller architecture is divided into four functional zones (Zone 1–Zone 4), each corresponding to specific circuit and control functionalities.

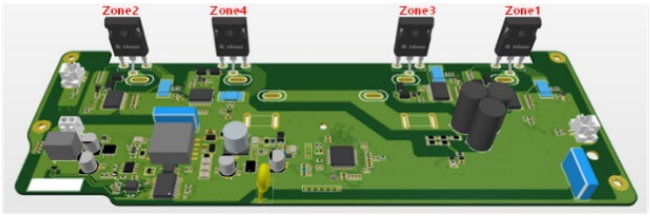

(a) 3D PCB design

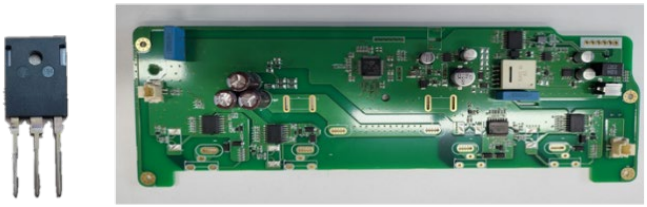

(b) SiC MOSFET device (c) fabricated PCB prototype

Fig. 6. Overview of the proposed four-channel PTC controller showing the 3D PCB layout, SiC MOSFET device, and the fabricated PCB prototype.

PTC Operation Circuit Analysis

A detailed circuit evaluation was conducted to investigate the interaction between resistive PTC loads and the parasitic capacitance of the PTC controller board under high switching frequencies. As shown in Fig. 7, thermal imaging revealed that the PCB temperature increased significantly faster at 20 kHz than at 10 kHz operation, even under a lower duty cycle. This non-linear temperature rise is attributed to elevated switching losses and cumulative heating effects caused by reduced cooling intervals, emphasizing the importance of effective thermal management and optimized PCB layout for ensuring long-term reliability. Measured switching waveforms in Fig. 8 further illustrate the transient behaviour of the SiC MOSFET under PTC load conditions. At turn-on, a pronounced current overshoot was observed, followed by a gradual reduction in the current slope. During turn-off, the drain–source voltage (V_{DS}) exhibited a slow rise, while the current level remained higher than

expected. This behaviour indicates possible energy recirculation through parasitic elements within the PTC load. These findings suggest that reducing parasitic inductance and capacitance in the PCB layout, together with careful gate-drive tuning, is critical to controlling switching transients, minimizing power loss, and improving the system's thermal stability.

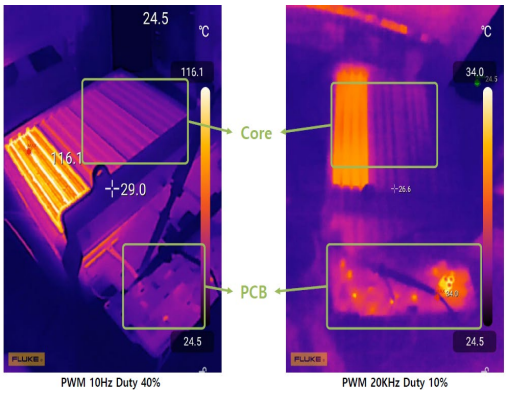

Fig. 7. PTC load operation with thermal imaging.

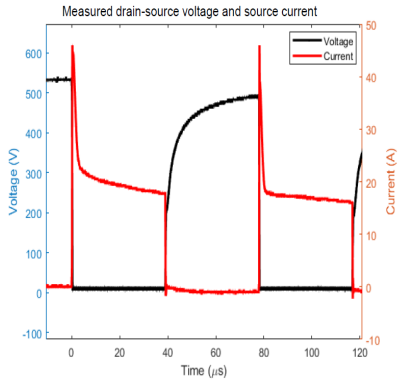

Fig. 8. Measured switching waveforms at the drain-source (V_{DS}) terminal of the SiC MOSFET.

PTC Load Modelling and Switching Analysis

Since the measured switching waveforms under PTC load conditions did not follow the typical turn-on and turn-off behaviour observed with purely resistive or inductive loads, a detailed load analysis was performed. As illustrated in Fig. 9, the PTC heating module consists of multiple ceramic elements that inherently introduce parasitic resistance, capacitance, and inductance into the switching loop. In each row of the PTC heat load module, six ceramic pieces act as distributed parasitic capacitances and resistances, with each piece connected through parasitic inductances.

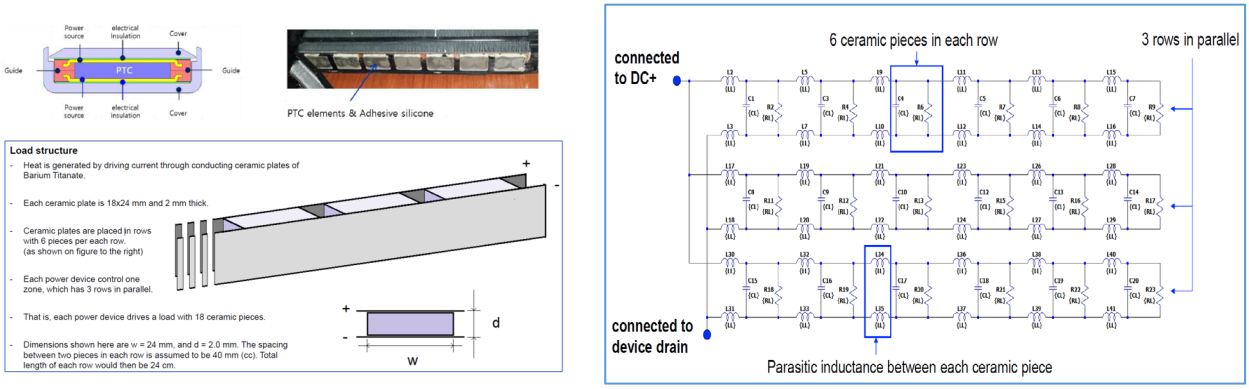

Fig. 9. PTC load structure (left) and simplified RC modelling of the PTC load circuit (right).

To capture these characteristics, the complex PTC load structure was represented using a simplified equivalent RC network model in Fig. 10. Through this modelling, load conditions were simulated using a 150 nF capacitor in parallel with a 200 Ω resistive element, representing the aggregated parasitic characteristics of the module. This equivalent model enabled quantitative analysis of transient overshoot currents, electromagnetic interference (EMI) behaviour, and energy loss distributions. The stored energy in the capacitor at 525 V was calculated to be 21 mJ. Total system losses were determined by subtracting the measured load dissipation from the total simulated input energy, including contributions from the DC-link capacitor. This approach isolates the energy dissipated within parasitic components and non-idealities in the circuit, which are not directly converted into useful heat by the PTC elements.

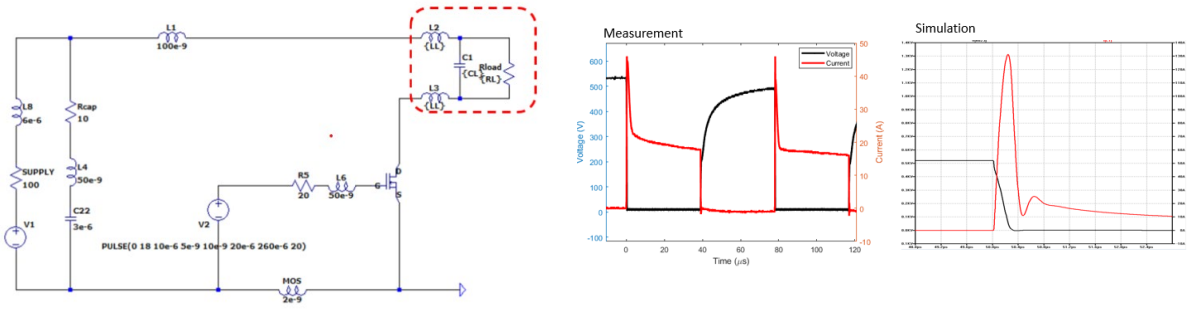

Fig. 10. Switching circuit with simplified PTC load model (left) and comparison of measured and simulated switching waveforms (right).

The simplified RC modelling of the PTC load accurately reproduced the measured switching waveforms, confirming that the parasitic resistance, capacitance, and inductance of the ceramic elements significantly influence the switching transients. The analysis highlighted three key factors for optimal system performance: (i) current overshoot during turn-on can be substantial and requires careful evaluation under varying temperature conditions, (ii) the DC-link capacitor selection must balance low ESR for efficiency with sufficient damping to suppress turn-off ringing, and (iii) accurate load modelling is essential to predict transient behavior and minimize energy losses within parasitic elements.

Acoustic Noise Testing and Evaluation

For the noise measurement, the experimental setup was established inside an acoustic chamber isolated from external disturbances. A microphone was positioned at a distance of 50 cm from the PTC heater, and the measurements were conducted under controlled conditions to ensure accurate evaluation of the generated acoustic noise. The measurement environment is illustrated in Fig. 11.

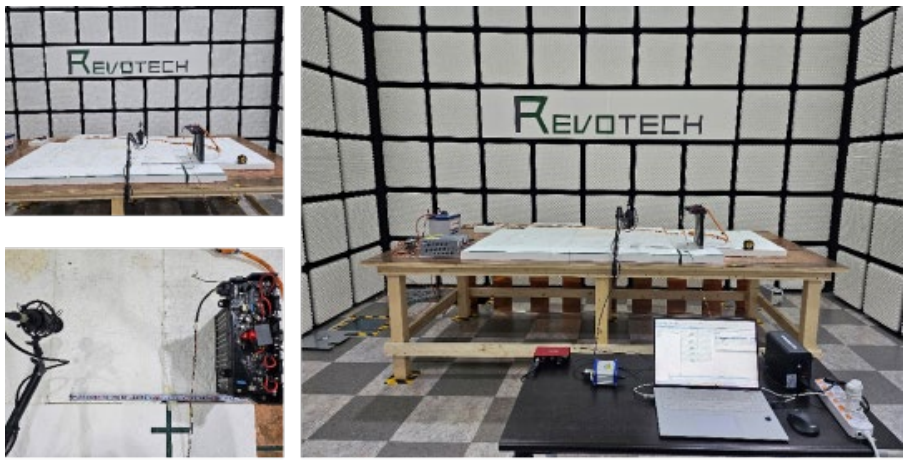

Fig. 11. Experimental setup for acoustic noise measurement.

The test results revealed that when the PTC controller was operated at switching frequencies of 100 Hz, 1 kHz, 10 kHz, and 15 kHz, the corresponding audible noise could be clearly perceived by the human ear. In contrast, when the switching frequency was increased to 100 kHz, the generated noise was indistinguishable from the background level, and no audible difference could be detected compared to the no-operation condition where the controller was not operating. This finding indicates that operating the PTC controller in the ultrasonic range can effectively suppress audible noise. Furthermore, the spectrogram shown in Fig. 12 confirms this observation: while distinct frequency components are visible in the lower frequency cases, the 100 kHz operation exhibits only broadband white noise similar to the no-operation condition, thereby validating the effectiveness of the proposed high-frequency switching strategy in eliminating perceptible acoustic noise.

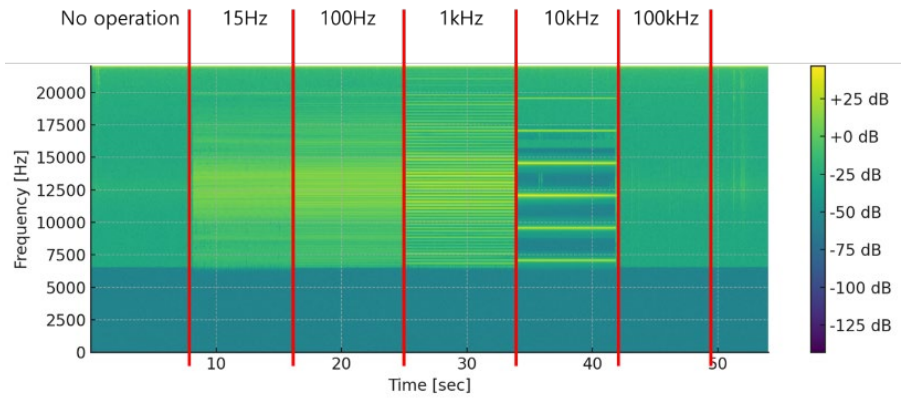

Fig. 12. Spectrogram of noise signals at different switching frequencies.

Conclusion

The switching performance and thermal stability of PTC controllers are influenced not only by the inherent advantages of SiC MOSFETs but also by the optimization of the entire system environment. To achieve strong temperature stability, it is crucial to carefully balance MOSFET conduction and switching losses with DC-link capacitor heating and electromagnetic interference (EMI) suppression. A proper trade-off among these factors is essential to ensure both high efficiency and long-term reliability. To prevent potential thermal runaway, the gate voltage and gate resistance must be selected with consideration of the device's gate–source capacitance and its impact on switching transients. In particular, controlling the turn-on current overshoot and mitigating turn-off ringing are key to reducing device stress and minimizing parasitic loss. In addition, the selection of the DC-link capacitor has a significant impact on overall system performance. While low-ESR capacitors can enhance efficiency, they may also increase the likelihood of oscillations during switching. Therefore, capacitor design should balance efficiency and oscillation suppression, with the potential inclusion of RC snubber circuits as an effective supplementary measure.

Finally, experimental results confirmed that when the switching frequency was raised to the ultrasonic range (e.g., 100 kHz), the PTC controller produced only broadband white noise indistinguishable from the no-operation condition, meaning that no audible sound could be perceived by the human ear. This demonstrates that the proposed design not only ensures thermal and electrical stability but also effectively eliminates acoustic noise, thereby enhancing passenger comfort in practical xEV applications.

Acknowledgement

This work was supported by the International Joint Technology Development Project (Global Cooperation Hub-type Joint R&D) under grant agreements No. P146500052 and No. P0026051, funded by the Korea Institute for Advancement of Technology (KIAT) through the Ministry of Trade, Industry and Energy (MOTIE), Republic of Korea.

References

[1] Albanna A., et al., "Performance comparison and device analysis Between Si IGBT and SiC MOSFET." presented in 2016 IEEE Transportation Electrification Conference and Expo (ITEC), IEEE, 2016, pp. 1–6. doi:10.1109/ITEC.2016.7520242.

[2] Ranstad P., et al., "An experimental evaluation of SiC switches in soft-switching converters," IEEE Transactions on Power Electronics, vol. 29, no. 5, pp. 2527–2538, May 2014.

[3] Hao X., et al., "Seasonal effects on electric vehicle energy consumption and driving range: A case study on personal, taxi, and ridesharing vehicles," Journal of Cleaner Production, vol. 249, article. 119403, 2020.

[4] Sadik D.P., et al., “Comparison of thermal stress during short-circuit in different types of 1.2-kV SiC transistors based on experiments and simulations,” IEEE Transactions on Industrial Electronics, vol. 68, no.3, 2608-2616, Mar. 2021.

[5] Lim, J.-K., et al., “Comparison of total losses of 1.2 kV SiC JFET and BJT in DC-DC converter including gate driver,” Materials Science Forum, vols. 679-680, pp. 649-652, Apr. 2011.

[6] Buffolo M., et al., “Review and Outlook on GaN and SiC Power Devices: Industrial State-of-the-Art, Applications, and Perspectives,” IEEE Transactions on Electron Devices, vol. 71, no. 3, 1344-1355, Mar. 2024.